Interferometric Spectro-imaging of Molecular Gas in Proto-Planetary Disks

Anne Dutrey and Stéphane Guilloteau
L3AB, Observatoire de Bordeaux

Paul Ho
Academia Sinica Institute of Astronomy and Astrophysics and Smithsonian Astrophysical Observatory

Proto-planetary disks are found to orbit around low and intermediate mass stars. Current theories predict that these disks are the likely sites for planet formation. In this review, we summarize the improvement in our knowledge of their observed molecular properties since PPIV. This is timely since a new facility, the Submillimeter-Array (SMA), has recently begun operation and has opened the submillimeter atmospheric windows to interferometry, allowing studies of warmer gas and dust in disks at subarcsecond resolution. Using results from the IRAM array and the SMA, we focus on two complementary main topics: 1) the determination of the physical structure of the disks from multi-transition CO isotopic analysis of high angular resolution millimeter interferometric data and 2) the observations of molecules other than CO (and isotopes), which enable investigations of the chemistry in proto-planetary disks. In particular, we emphasize how to handle the available data to provide relevant constraints on the thermal, physical and chemical structure of the disks as a function of radius, within the current limitations in sensitivity and angular resolution of the existing arrays. These results suggest the importance of photo-dissociation effects and X-ray heating. They also reveal unexpected results, such as the discovery of non-Keplerian rotation in the AB Aur disk. We also discuss how to extrapolate these results in the context of the tremendous capabilities of the ALMA project currently under construction in Chile.

1. INTRODUCTION

In the last fifteen years, observations from the optical up to the millimeter wavelength domains have revealed that low and intermediate mass stars of ages around a million years, such as TTauri and Herbig Ae stars, are surrounded by circumstellar disks. These disks are often called "proto-planetary" because they still contain enough original material (from the parent cloud) to form giant planets. Indeed, although dust is the easiest tracer of proto-planetary disks, molecules represent more than 70 % of the total mass in disks. H_2, which does not deplete on dust grains, is by far the most abundant molecule in disks but it remains difficult to observe because of the lack of a dipole moment. Even if a few direct H_2 detections are now possible, the observed H_2 lines mainly trace the warm gas located in the inner disks (R$<$ 10-20 AU), while, in many cases, disks are known to extend out to several 100 AU. These outer regions, which may even contain most of the mass, are cold and can only be characterized by molecules having rotational lines at low energy levels and detectable with large millimeter and sub-millimeter interferometers. After H_2, CO is the most abundant molecule (even if it can deplete on dust grains) and its lowest rotational lines are easily excited by collisions with H_2 in disks. Only heterodyne arrays give the sensitivity, resolving power and spectral resolution needed to map cold molecular disks. In the last ten years, millimeter spectroscopic studies of disks have shown that they are in Keplerian rotation. More recently, the SMA (*Ho et al.*, 2004) has opened a new the era of sub-millimeter interferometry, while the IRAM Plateau de Bure interferomter (PdBI) routinely provides images of 0.6" resolution at 1.3mm. Since PPIV, observations of molecular disks have considerably improved, and mm/submm arrays have provided many new direct constraints on physical and chemical structure of disks which could not be addressed by disk continuum observations.

In this review we focus on the recent molecular results obtained with the SMA and the IRAM array. We summarize in Section 2 the sensitivity which can be achieved by observing CO transitions in disks with the PdBI and the SMA. We also calculate the brightness temperature for transitions J=1-0 up to J=3-2 and describe new methods of analysis for interferometric data. In Section 3, we present the CO disk properties as inferred from SMA and IRAM array observations. Then Section 4 is dedicated to new results for some specific disks because they provide new quantitative information on the disk physics since PPIV. Particular attention is given to the observation of molecular chemistry in Section 5. Then we conclude by presenting the sensitivity of ALMA. This paper focusses on line data and outer disks only. In these proceedings, more information on continuum emission can be found in the chapters by *Testi et al.*, and on chemistry by *Bergin et al.*

2. MOLECULAR LINE FORMATION AND DISK MODELS

The line formation process in proto-planetary disks is complicated because of the combination of strong velocity, temperature and density gradients. The regular pattern of rotational motions provides a direct link between the projected velocity and position in the disk, a property which provides some effective super-resolution, under the guidance of an applicable model. In addition, proto-planetary disks have two specific properties which make the derivation of physical parameters from observations particularly robust and relatively simple:

1. Power laws are good approximations for the radial dependence of many physical quantities
2. As a result, molecular column densities can be derived from the observation of a single (partially optically thin) transition.

However, radiative transfer models are required to estimate the line brightness distribution as a function of projected velocity. This implies the use of dedicated codes, whose precision should be matched to the sensitivity of the observations to be analyzed. Such detailed models have become necessary only because the observations now provide sufficient sensitivity. In this section, we describe the available tools and their use.

2.1. Disk Description

Disks models (such as those described in *Dutrey et al.*, 1994) are usually based on the description of *Pringle* (1981): a geometrically thin disk in hydrostatic equilibrium with sharp inner and outer edges. Temperature, velocity and surface density assume power law radial dependencies:

For the kinetic temperature: $T(r) = T_o(r/r_o)^{-q}$

the surface density: $\Sigma(r) = \Sigma_o(r/r_o)^{-p}$

and the velocity: $V(r) = V_o(r/r_o)^{-v}$, with $v = 0.5$ for Keplerian disks.

We start by the simplest approach which assumes power law dependencies versus radius. This is of course appropriate for the velocity, and power laws have been shown to be a good approximation for the temperature distribution (e.g., *Chiang and Goldreich*, 1997). Using power laws for the surface density is more debatable. It is often justified for the mass distribution based on the α prescription of the viscosity with a constant accretion rate, but may not be applicable to any arbitrary molecule. Given the limited spatial dynamic range provided by current (sub-)millimeter arrays, more sophisticated prescriptions are not warranted.

Since the disks are assumed to be in hydrostatic equilibrium, the volume density is given by

$$n(r,z) = n(r,0)e^{-\left(\frac{z}{H(r)}\right)^2}$$

where the mid-plane density $n(r,0)$ and the hydrostatic scale height $H(r)$ are given by:

$$n(r,0) = \frac{\Sigma(r)}{\sqrt{\pi}H(r)} = n_o(r/r_o)^{-s}$$

$$H(r) = \sqrt{\frac{2kr^3T(r)}{GM_*\overline{m}}} = h_o(r/r_o)^h$$

and also follows power laws with $h = 1 + v - q/2$ and $s = p + h = p + 1 + v - q/2$. G, M_* and $\overline{m}$ are the gravitational constant, the stellar mass (the disk is not self-gravitating) and the mean molecular weight, respectively.

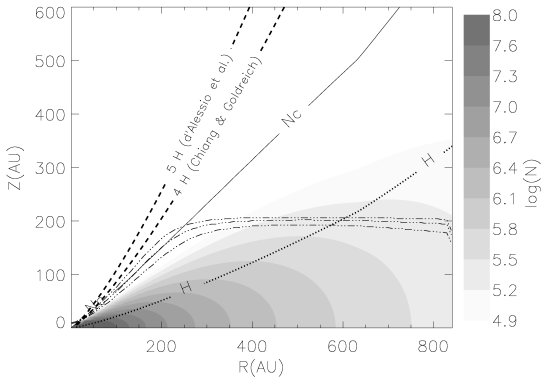

Fig. 1.— Density structure of the DM Tau disk, with the critical density for thermalization of the J=2-1 transition, N_C, indicated, as well as the $\tau = 0.5, 1, 2$ opacity curves (dash-dotted lines). The super-heated layers of the *Chiang and Goldreich* (1997) model and of those of *D'Alessio et al.* (1997, 1999) are also indicated. From *Dartois et al.* (2003).

The definition given above implies that $H(r) = \sqrt{2}c_s/\Omega$ (where c_s is the sound speed and Ω the angular velocity). Other groups take $H(r) = c_s/\Omega$ (*D'Alessio et al.*, 1998; *Chiang and Goldreich*, 1997). As a consequence the scale height given in this description is $\sqrt{2}$ larger, and this must be properly taken into account in comparisons.

Fig. 1 presents the density structure of a representative disk, the DM Tau disk, with characteristic curves overlaid on it. For any given molecular line, two curves are especially important: the height at which the density for thermalization is reached, and the height at which an opacity of order 1 is obtained. By comparing the two, one can readily derive whether non-LTE effects have to be considered or not. These curves are given for the CO J=2-1 transition in Fig. 1, using a depletion factor of ten, showing that this transition remains thermalized throughout the disk, as $\tau = 1$ curve is below the critical density line. Note that higher CO lines, J=3-2 and above, are more optically thick and have higher critical densities, and therefore may be sensitive to non-LTE effects.

2.2. Analysis of Thermalized Lines

For the analysis of thermalized lines a ray tracing code integrating the radiative transfer equation step by step along the line of sight is enough, although care must be taken to use sufficient resolution for the extreme velocities, which originate from the inner parts of the disk.

The brightness temperature T_b of a proto-planetary disk can be easily expressed as a function of radius r for a face-on disk. In the optically thick case

$$T_b(r) = T(r) = T_o \times (r/r_o)^{-q} \quad (1)$$

while in the optically thin case

$$T_b(r) = \tau.T(r) \quad (2)$$

which, for the $J+1 \rightarrow J$ transition of a linear molecule, is

$$\begin{aligned} T_b(r) &= \frac{8\pi^3}{3h}\mu^2 \cdot \frac{(e^{-\frac{E_J}{kT(r)}} - e^{-\frac{E_{J+1}}{kT(r)}})}{Z\Delta V} \\ &\quad (2J+1)\frac{X(r)}{m_{H_2}\overline{m}}T(r)\Sigma(r) \\ T_b(r) &= \frac{8\pi^3}{3h}\mu^2 \cdot e^{-\frac{E_J}{kT(r)}}\frac{(1-e^{-\frac{h\nu}{kT(r)}})}{Z\Delta V} \\ &\quad (2J+1)\frac{X(r)}{m_{H_2}\overline{m}}T_o\Sigma_o(r/r_o)^{-(p+q)} \quad (3) \end{aligned}$$

where X is the molecular abundance relative to H_2 (Σ being a mass surface density in this formula) and Z is the partition function. The local linewidth ΔV is given by $\Delta V = \sqrt{v_{th}^2 + v_{turb}^2}$, where v_{th} is the thermal line-width and v_{turb} a turbulent term usually of order $\simeq 0.1$ km.s^{-1} (*Dartois et al.*, 2003).

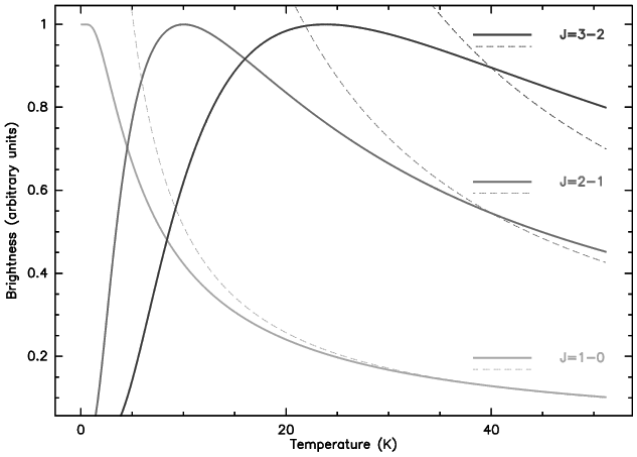

Fig. 2.— Brightness, given in arbitrary units, versus kinetic temperature for CO lines J=1-0, J=2-1 and J=3-2 in a Keplerian disk. Both a high temperature approximation and exact formula are drawn. Only the J=1-0 transition appears well represented by the high temperature approximation in the whole disk (from *Dartois et al.*, 2003).

At high enough temperature, the expression can be simplified. The partition function is $Z \simeq \frac{kT}{hB}$, and the Rayleigh Jeans approximation , $h\nu << kT$, can be used. For the J=1-0 transition, equation 3 shows that

$$T_b(r) \propto X(r)\Sigma(r)/T(r)$$

if the line-width is constant or

$$T_b(r) \propto X(r)\Sigma(r)/T(r)^{3/2}$$

if the line-width is thermal. Fig. 2 compares the approximation with the exact formula.

For higher transitions, a similar asymptotic behavior is obtained if $E_{J+1} << kT$, but at lower temperature the exponential term in Eq.3 plays a significant role. For typical temperatures of proto-planetary disks, the J=2-1 transition brightness is $T_b(r) \propto X(r) \cdot \Sigma(r)$ to first order.

For inclined disks, the above treatment is a simplification indicating the first order behavior as a function of radial distance from the star. Because of the velocity shear due to the disk rotation, the line opacity is a complex function of the position and projected velocity, but the general trend remains.

For the CO abundances found in disks (*Dutrey et al.*, 1997), the first rotational transitions of ^{12}CO are optically thick throughout the disk. It is convenient to call the disk layer where ^{12}CO J=2-1 reaches an opacity of ~ 1 along the line of sight as the "CO surface" of the disk. Rarer CO isotopologues appear partially optically thin in the outer regions, but remain optically thick in the inner parts. In this case, a single line can provide measurement of both the temperature and the (molecular) surface density, provided the power law distribution holds everywhere. Optically thick lines are direct tracers of the kinetic temperature at $\tau \simeq 1$ along the line-of-sight. This property can thus be used to sample not only the radial but also the vertical temperature gradient in the disk. This method is illustrated by Fig. 3 for a pole-on disk and was first developed by *Dartois et al.* (2003) in the case of the DM Tau disk (see also Section 2.5).

2.3. Sensitivity of mm/sub-mm arrays

Many gas disks are large enough (outer radius $R_{out} \simeq 200 - 800$ AU) to allow mm/sub-mm arrays to measure the molecular brightness distribution versus radius. To understand the limitation of the measurements, it is important to compare the expected line brightness with the array sensitivity.

Fig. 4 presents the expected brightness temperature as a function of radius for the J=2-1 and J=3-2 transitions of the CO isotopologues, and of the dust emission at the corresponding frequencies, and compare them with the sensitivity of the SMA and Plateau de Bure interferometers, estimated using the canonical values in system temperature, efficiency, etc... Note that although the continuum sensitivities could be improved by increasing the detector bandwidth, this is not the case for the spectral lines where the bandwidth is limited by the intrinsic line width. Only better receivers or more collecting area can improve the situation in this case.

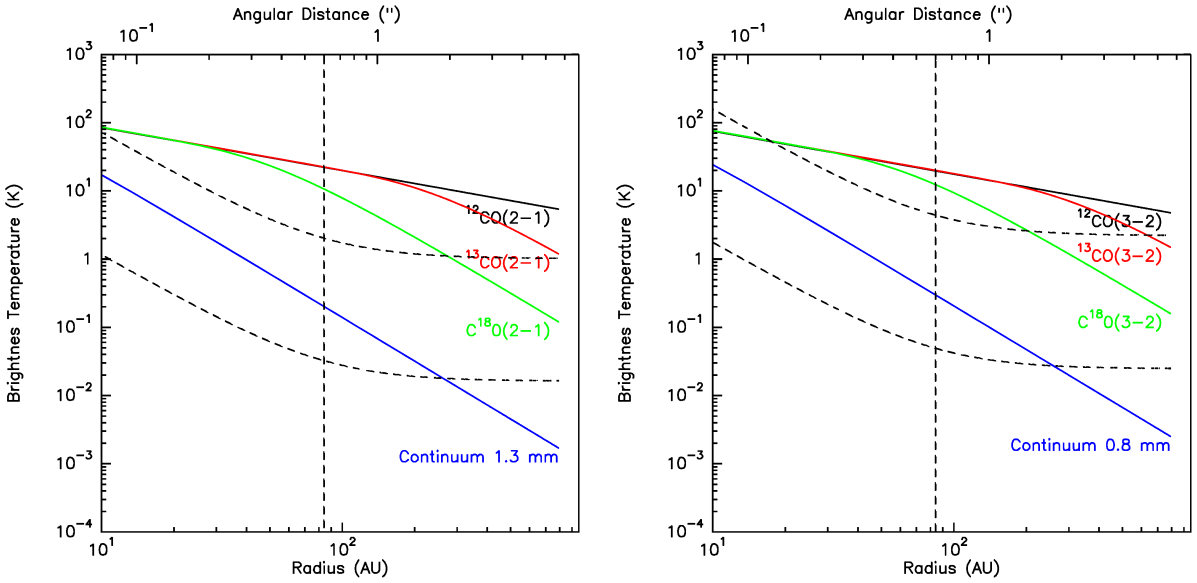

Fig. 4.— Left: Brightness temperature for CO (and isotopomers) in J=2-1 transition for a Keplerian disk orbiting a central object of $\sim 1\,M_\odot$ (thick lines) compared to the sensitivity of the IRAM Plateau de Bure array (dashed lines). Right: Same for the SMA in the transition J=3-2. We assume LTE conditions which are valid for J=2-1 but the J=3-2 line is not necessarily thermalized everywhere. This curve is only an upper limit to the expected signal. The angular resolution is here $0.6''$. This corresponds to the best resolution obtained so far. The diagram has been calculated for a TTauri disk located at the Taurus distance: 140 pc.

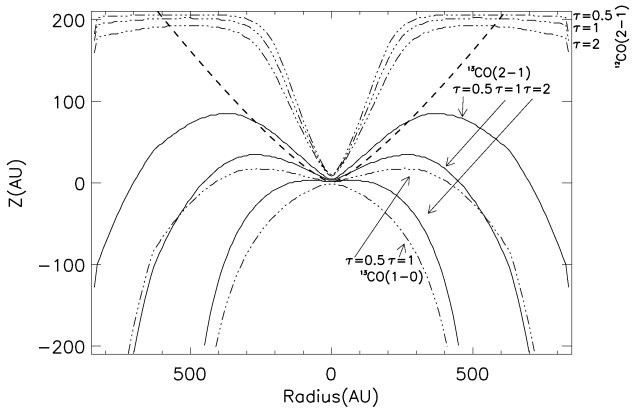

Fig. 3.— Surface at which the opacity along the line of sight reaches one for the various CO isotopes overlaid on the density structure (grey scale). This figure assumes the canonical density of DM Tau disk (taking into account a depletion factor of 10 for the CO abundance). Assuming this disk to be representative of its category, this shows that transitions above the J=3-2 are not thermalized, at least in the outer layer. (From *Dartois et al.*, 2003).

The brightness temperature clearly shows the two expected regimes for the partially optically thin transitions: $T_b(r) = T_k(r)$ at small radii, and $T_b(r) \propto X(r)\Sigma(r)$ at large radii. Depending on the relative importance of the two regimes, the analysis of the observations will suffer from different limitations. The temperature determination will be difficult if insufficient resolution is available, while the surface density determination is limited by the low S/N in the outer regions. The apparent sizes will be largely dependent on the optical depth, rather than on the true outer radius. This is the reason why the (apparent) observed size of a dust disk always appears smaller than the size of its ^{12}CO emission. Fortunately, for both the SMA and the PdBI, many CO disks can be observed with a similar level of sensitivity.

2.4. UV plane analysis and χ^2 minimization techniques

Fig. 4 clearly shows that sensitivity is a limitation even with the best arrays available so far. This problem is further amplified by the limited UV coverage due to the small number of antennas in all existing mm/sub-mm arrays. The IRAM array has 6 antennas of 15-m diameter while the SMA has 8 antennas of 6-m diameter This limited UV coverage implies significant sidelobe levels in the dirty images, and deconvolution is required to remove them. However, deconvolution is a non-linear process which increases the noise level, specially for the case of weak extended structures. As a consequence, comparing disk models to CLEANed images is currently a method which remains inaccurate. With 9 antennas of 6-m diameter and 6 of 10.4-m diameter, CARMA will improve the synthesized beam issue, but remain sensitivity limited. With 50 antennas of 12-m diameter, these problems will become much less significant with ALMA since the sampling of the UV plane will be significantly higher (1225 instantaneous baselines). The addition of the ACA to ALMA will also improve the

sampling of the short spacings, which can be important for the sub-mm data.

Accordingly, the optimal way to analyze the data is to compare directly the "raw" data, i.e. the observed visibilities, with the predicted visibilities from the model images. Weighting each visibility data point by its (known) thermal noise allows the definition of a least square distance between the model and the data, in the usual χ^2 sense:

$$\begin{aligned}\chi^2 &= \Sigma_n\Sigma_i(Re(mod_{i,n}) - Re(obs_{i,n}))^2 \times W_i \\ &+ \Sigma_n\Sigma_i(Im(mod_{i,n}) - Im(obs_{i,n}))^2 \times W_i \quad (4)\end{aligned}$$

where $Re(a)$ and $Im(a)$) are the real and imaginary parts of the visibility a, and $a_{i,n}$ is the visibility i for velocity channel n. The weight W_i is derived from the system temperature T_{sys}, the spectral resolution $\Delta\nu$, the integration time τ, the effective collecting area of one antenna A_{eff} and the loss of efficiency introduced by the correlator η: $W_i = \frac{1}{\sigma_i^2}$ with $\sigma_i = \frac{\sqrt{2}kT_{sys}}{A_{eff}\eta\sqrt{\tau\Delta\nu}}$.

Since, for the LTE case, the model images are characterized by a reasonably small number of parameters (x_0, y_0, PA, $V_{\rm LSR}$, ΔV, $R_{\rm out}$, $V_0, v, T_0, q, \Sigma_0, p$ and i (the inner radius being in general not significantly constrained because of the lack of sensitivity (see Fig. 4), χ^2 minimization techniques can be used to determine the best model parameters and, ideally, their error bars. This was first used by *Guilloteau and Dutrey* (1998), using a simple grid-mapping to find the best model for CO in DM Tau. This is however slow, and does not properly consider the coupling between the parameters in the error determination. These two limitations have been recently overcome by *Piétu et al.* (2005), who used a more sophisticated and faster minimization routine, which takes into account the coupling between the parameters (but not the skewness of the distribution, i.e. asymmetric errorbars). Analysis of the data inside the UV plane with χ^2 minimization is becoming a standard procedure (although the derivation of error bars is not always performed), and a similar method has been recently applied by *Qi et al.* (2004) to the SMA CO J=3-2 data of TW Hya (see also Section 4.2). Neither method includes the systematic bias which may be introduced by using an inappropriate disk model, though.

2.5. An example: DM Tau

Because it is isolated from the nearby molecular clouds, DM Tau was among the first single stars around which a bona-fide proto-planetary Keplerian disk was detected (*Guilloteau and Dutrey*, 1994). This T Tauri star, located at 140 pc, is surrounded by a large CO disk of $\sim$ 800 AU. It was the first object for which the method of UV analysis described above was developed, allowing the first measurement of its stellar mass ($M_* = 0.5\,{\rm M}_\odot$, *Guilloteau and Dutrey*, 1998). Because of its large CO disk, it was also the first object on which a multi-isotope study of CO was performed (*Dartois et al.*, 2003). Since the ^{13}CO J=1-0 and J=2-1 sample different disk layers, a global analysis of

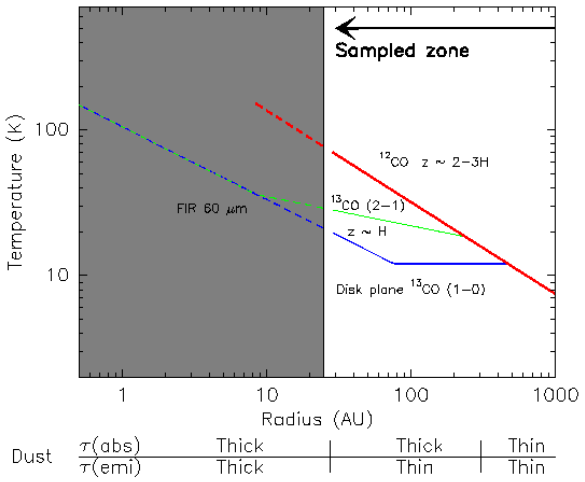

Fig. 5.— Vertical temperature gradient in the DM Tau disk inferred from multi-transition, multi-isotope CO analysis (from *Dartois et al.*, 2003)

these lines permit the derivation of the vertical kinetic temperature gradient. In the case of DM Tau, the measured gradient is in agreement with predictions from models of disks externally heated by their central star (e.g. *D'Alessio et al.*, 1999). The mid-plane is cooler ($\sim$ 13 K) than the CO disk surface ($\sim$ 30 K at 100 AU). This appears in the region of the disk where the dust is still optically thick to the stellar radiation while it is already optically thin to its own emission, around $r \sim 50 - 200$ AU in the DM Tau case. Beyond $r \geq 200$ AU where the dust becomes optically thin to both processes, the temperature profile appears vertically isothermal.

Fig. 5 also shows that a significant fraction of the DM Tau disk has a temperature which is below the CO freeze out point (17 K) but there remains enough CO in the gas phase to allow the J=2-1 line of the main isotope to be optically thick. This is also the case for most of the sources discussed here, and there is no satisfactory explanation of this chemical puzzle, so far.

2.6. Subthermal Excitation

The previous sections show how thermalized transitions can be analyzed using a simple power law model for the temperature, and show that the temperatures derived from isotopologues can provide insights into the radial and vertical temperature structure of the disk. If the same analysis is used for a transition which remains sub-thermally excited (in the regions where its opacity is > 1), such an analysis will yield the excitation temperature of the line instead of the kinetic temperature. If all lines of the molecule shared the same excitation temperature (i.e. if $T_{\rm ex} = T_{\rm rot}$, the rotation temperature), the molecular column density would still be correctly determined. In general, though, $T_{\rm ex}$ will decrease with the energy levels, and the above assumption will underestimate the partition function, leading to a slight

underestimation of the column density.

A more accurate determination of the column density requires solving the coupled equations of statistical equilibrium and radiative transfer. This introduces 4 additional complexities:

1. The disk temperature structure must be known
2. The disk density structure must be known
3. The location of the molecules within the disk must be known, and
4. the coupled equations must be solved to sufficient accuracy

The last complexity is actually the less difficult to solve. For this purpose, two kinds of models are currently being used:

1. Approximate solutions based on escape probability and 1-D radiative transfer, such as those developed by *Piétu et al.* (2006).
2. Full 2-D Monte-Carlo radiative transfer codes (*Hogerheijde and van der Tak*, 2000; *Pavlyuchenkov and Shustov*, 2004)

The first method remains fast enough for use in χ^2 minimization routines, the escape probability technique being only marginally slower than a simple LTE approximation. The second method is in theory more accurate from the point of view of the radiative transfer, provided the Monte-Carlo noise is adequately controlled, but current implementations are too slow for use in χ^2 minimization. Furthermore, it should be stressed that the gain in accuracy is not necessarily significant: the main limitation in accuracy remains currently in the interferometric observations, because all molecular lines (except those of ^{12}CO) are relatively weak. Moreover, all techniques suffer from the required a priori knowledge of the temperature and density structure of the disk, and of the localization of the molecules within this structure. The related uncertainties are often much larger than those introduced by the approximation made to solve the coupled statistical and radiative transfer equations.

For the disk structure, two methods are presently in use.

1. The gas kinetic temperature is determined from the CO line analysis, and the radial density distribution from the fit of the millimeter continuum images. This is the method used by Dutrey, Guilloteau and collaborators.
2. The kinetic temperature and density structures are determined by modelling the Spectral Energy Distribution (and in some cases, interferometric dust map) of the dust disk with a model similar to those of *Chiang and Goldreich* (1997) or *d'Alessio et al.* (1998). This method supposes 1) a dust grain distribution and composition and 2) that dust and gas have the same kinetic temperature, a good approximation over the whole disk (with the exception of the disk atmosphere where the density is low). This method was recently used to determine the best physical parameters of the gas disk orbiting TW Hya by *Qi et al.* (2004).

In both methods, hydrostatic equilibrium is assumed. The largest source of uncertainty remains the radial density distribution, which is coupled to the dust properties.

Finally, the localization of the molecules within the disk remains an unsolved problem. One can either assume full vertical mixing, or use vertical distributions provided by chemical models. Given all the combined uncertainties, it remains unclear whether a full non-LTE analysis yields more sensible results than those provided by the simple $T_{\rm rot}$ approximation.

3. PROTO-PLANETARY DISKS PROPERTIES

The first extensive detailed analysis of CO emission from disks around T Tauri and HAeBe stars using the above methods was performed by *Simon et al.* (2000). They used the ^{12}CO J=2$\rightarrow$1 emission to characterize the disks around 12 stars, showing the existence of large (often > 300 AU) disks and demonstrating unambigously the Keplerian nature of the rotation. More recently, *Piétu et al.* (2006) have extended the CO isotopologue line analysis performed for DM Tau to a small sample of TTauri (LkCa15) and Herbig Ae stars (MWC480, AB Aur and HD34282).

Together with other studies of HAeBe stars by *Mannings and Sargent* (1997, 2000), this allows some robust conclusions to be reached:

1. Large disks (CO outer radius of $\sim 200 - 1000$ AU) exist.
2. The intrinsic linewidths are small, with a non-thermal component of order $\sim 0.1 - 0.2$ km.s^{-1}.
3. All disks studied so far are in Keplerian rotation (with the exception of AB Aur which is described in Section 6). Since the mass of the disks is negligible, χ^2 minimization as those described in the section above allow direct measurements of the stellar mass (see also Fig. 6).
4. For both Herbig Ae and (classical) TTauri disks, the kinetic temperature at the CO disk surface (defined as the surface where $\tau \simeq 1$ is reached for the ^{12}CO J=2-1 transition) is in agreement with the model of flared disks heated by the central star, $T(r) \propto r^{-0.6}$.
5. Multi-line, multi-isotope analysis of CO reveal the existence of a vertical temperature gradient in outer disks which seems compatible with disk models, with disk-mid planes cooler than CO surfaces.
6. Disks orbiting around Herbig Ae stars are hotter than those found around TTauri stars. ^{13}CO observations

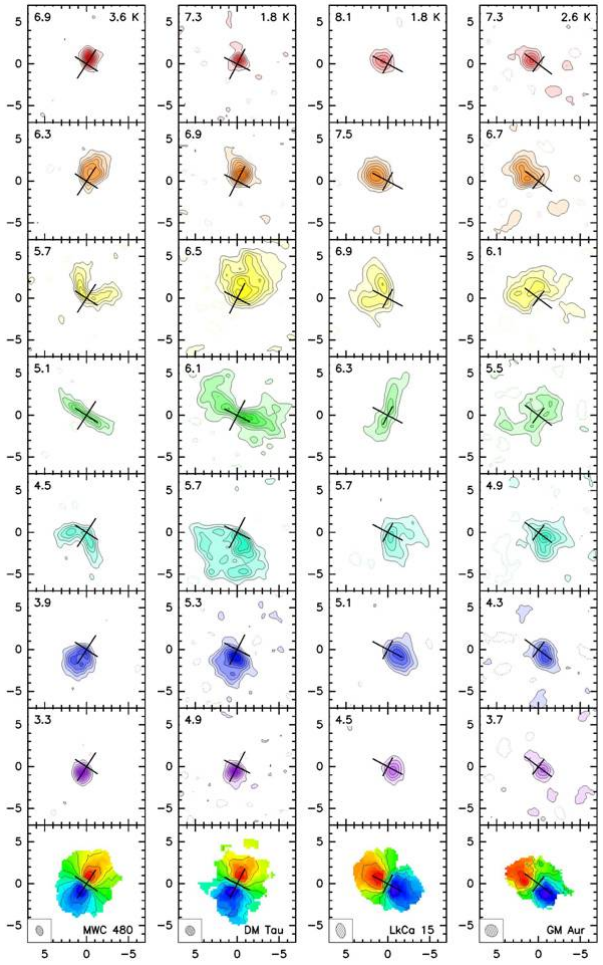

Fig. 6.— CO J=2-1 channel maps of disks around TTauri and Herbig Ae stars in Taurus-Auriga, observed with the IRAM array. These objects are isolated from their parent clouds. The channel patterns appear very similar from one disk to another. The analysis of the kinematics show that all these disks are in Keplerian rotation. Because of the velocity gradient and to the limited local line-width, only a small fraction of the disk contributes to the line emission in each velocity channel. From *Simon et al.* (2000).

also reveal that the temperature close to the disk mid-plane is larger and above the temperature of freeze-out of CO.

7. The degree of CO depletion clearly decreases with the effective temperature of the star, with CO being essentially undepleted in AB Aur, demonstrating that sticking onto dust grains plays a significant role in the depletion process.

8. Beyond a radius of $\sim$ 150 AU, outer disks orbiting TTauri stars have a temperature which is below 17 K, the CO freeze-out temperature. However, a significant amount of CO is still present (optically thick ^{12}CO J=2$\rightarrow$1 line) even at these low temperatures. This remains to be explained by chemical models.

9. Finally, when both ^{13}CO and ^{12}CO data are existing, the outer radius derived from ^{13}CO is smaller than the one derived from ^{12}CO. The differences are consistent with the behavior expected from selective photo-dissociation due to self-shielding.

Table 1 summarizes the known properties of outer disks inferred by mm and sub-mm arrays, so far. The properties above apply to classical T Tauri stars (CTTS) or HAe stars. In addition, *Duvert et al.* (2000) searched for disks around weak-lined T Tauri stars (WTTS). No bona-fide WTTS showed significant ^{12}CO emission, and the only disk found was around V836 Tau, a star which displays characteristics intermediate between Class II and Class III objects. The disk was unresolved, the observations indicating a radius $\simeq$ 120 AU. These observations, though statistically not significant, suggest that most of the outer disk disappears on the same time scale as the inner disk traced by the near-IR excess.

Table 1: Typical values for proto-planetary disks around T Tauri stars

Physical Parameter	Ref.Value	exponent
Outer radius	(AU)	-
R_{out}	200-1000	-
Turbulent line-width	(km s^{-}1)	
Δv	$\sim 0.1 - 0.2$	-
Column Density[1]	(g cm^{-2})	
$\Sigma(r) = \Sigma_{100} \times (r/100\mathrm{AU})^{-p}$	0.8	~ 1.5
Kinetic Temperature[2]	(K)	
T(r) = $T_{100} \times (r/100\mathrm{AU})^{-q}$	~ 30	~ 0.6
Velocity law[3]		0.53
V(r) = $V_{100}(r/100\mathrm{AU})^{v}$	-	$\pm$0.01

[1]: Of gas+dust, assuming a gas to dust ratio of 100.
[2]: T_{100} corresponds to the CO surface (J=2-1 line).
[1+2]: values taken from *Dartois et al.* 2003.
[3]: From *Simon et al.* 2000.

Finally, one should emphasize that interferometric observations of spectral lines do provide with high accuracy two parameters of the disk geometry: the position angle and, more importantly, the inclination, which is essential for the modelling of the SED.

4. SOME INTERESTING CASE STUDIES

The properties derived above for the disks of T Tauri and HAe stars are not necessarily representative of all stars. In particular the disk size is likely biased towards large values because the large disks provide the stronger emissions. Furthermore, the initial studies have focussed on objects well isolated from molecular clouds, in order to avoid confusion with the emission from the molecular cloud.

Indeed, recent results have revealed stars with atypical disk properties. We focus in this section on three well-known stars. AB Aur is considered as the proto-type of

the Herbig Ae star. TW Hya is the closest (and among the oldest) T Tauri star surrounded by a disk and BP Tau is considered, from optical observations, as the reference for a Classical T Tauri star surrounded by an active accretion disk. Thanks to the ability to trace directly the gas component and the disk kinematics, the mm/submm interferometric observations provide information which are in two cases, at least, in apparent contradiction with the simple picture obtained from optical observations.

4.1. AB Aur

In many aspects, AB Aur is taken as the proto-type of the Herbig Ae star. The star is an A0 star of $\sim 10^6$ years. Modelling of the SED shows that the star is a Group I source having a flared disk *(Meeus et al.*, 2001). It is also surrounded by a large reflection nebula *(Grady et al.*, 1999) extending up to ~ 10000 AU (Fig. 7, top). More recently, using the Subaru telescope, *Fukagawa et al.* (2004) found that at medium scale ($\sim 100-500$ AU) the material around the star presents a spiral pattern. *Semenov et al.* (2004), using the IRAM 30-m and Plateau de Bure interferometer, have shown that AB Aur is surrounded by a large envelope and a circumstellar disk traced by HCO^+.

4.1.1. PdBI Data

Recent sub-arcsecond images of AB Aur obtained by *Piétu et al.* (2005) with the IRAM Plateau de Bure interferometer in the isotopologues of CO, and in continuum at 3 and 1.3 mm reveal that the environment of AB Aur is very different from the proto-planetary disks observed so far with mm arrays. These observations also allow the authors to trace the structure of the circumstellar material in regions where optical and IR mapping is impossible because of the emission from the star itself.

In the top left panel of Fig. 7, the HST image from *Grady et al.* (1999) is given in grey scale while contours correspond to the thermal dust emission observed at 1.3 mm by *Piétu et al.* (2005) (the cross shows the star location). The mm continuum emission is not centrally peaked but is dominated by a bright, asymmetric ("spiral-like") feature at about 140 AU from the central star. Little emission is associated with the star itself.

The molecular emission, shown on bottom of Fig. 7, reveals that AB Aur is surrounded by a very extended flattened low mass gaseous structure ("disk") which is also not centrally peaked. Bright molecular emission is also found towards the continuum asymmetry. The large scale molecular structure suggests the AB Aur "disk" is inclined between ~ 25 and 35 degrees. The significant asymmetry of the continuum and molecular emission prevents an accurate determination of the inclination of the inner disk part. Surprisingly, the analysis of the CO line kinematics reveal that the disk rotation is non Keplerian, the exponent of the velocity law differing from 0.5 at the 10σ level (0.40 ± 0.01).

4.1.2. SMA Analysis

AB Aur has also been observed in the ^{12}CO J=3-2 line and continuum at 0.8 mm with the SMA by *Lin et al.* (2006). The dust emission is not centrally peaked but exhibits a lower surface density in the center. This is clearly seen on bottom of Fig. 7. The Subaru Near-Infrared image has been superimposed to the SMA continuum data (from *Lin et al.*, 2006). The sub-mm continuum emission is dominated by bright asymmetric spots which follow the spiral pattern visible in the Near-Infrared images.

Contrary to the continuum, the ^{12}CO J=3-2 observations peak at the stellar position. Moreover, in several velocity channels, the CO J=3-2 traces the innermost spiral arm seen in the NIR. The kinematics of the ^{12}CO data cannot be fitted by Keplerian rotation and the CO emission which follows the innermost spiral arm exhibits outward radial motions.

4.1.3. Comparison

It is clear that both SMA and PdBI data reveal that the circumstellar material presents many departures from a symmetric structure. In particular, both sets of data indicate that

1. spiral-like features are observed as in the Near-Infrared,
2. there is a clear (and large) departure from Keplerian rotation, and
3. at mm/sub-mm wavelengths, the inner disk has been cleared or, at least, exhibits a lower column density than the outer disk.

The interpretation remains however unclear. Using "standard" dust properties to derive the disk mass, the disk is not sufficiently massive to be unstable against its own gravity. Although dust absorption coefficients are in general rather uncertain in disks, making mass estimates quite unreliable, in this case the disk mass is corroborated by the CO abundances. This disk mass appears consistent with a normal CO abundance for the Taurus region. As the disk of AB Aur is warm enough (about 30 K in the spiral regions), it is indeed expected that CO does not deplete onto grains.

One possibility would be the formation of a planet or low mass companion in the inner disk. This is likely a possible explanation for the inner hole, but it remains unclear whether the spiral structure and strong departure from a Keplerian rotation can be sustained at such large distances from the perturbing object.

The other possibility would be that it is still in an early phase of star formation in which the Keplerian regime is not yet fully established. The latter interpretation is supported by the existence of a large envelope around AB Aur, and is reinforced by the fact that the dust observed at mm wavelengths appears less evolved than in most proto-planetary disks.

These observations alone do not allow a definite answer and more modelling of the first phase of disk and planet

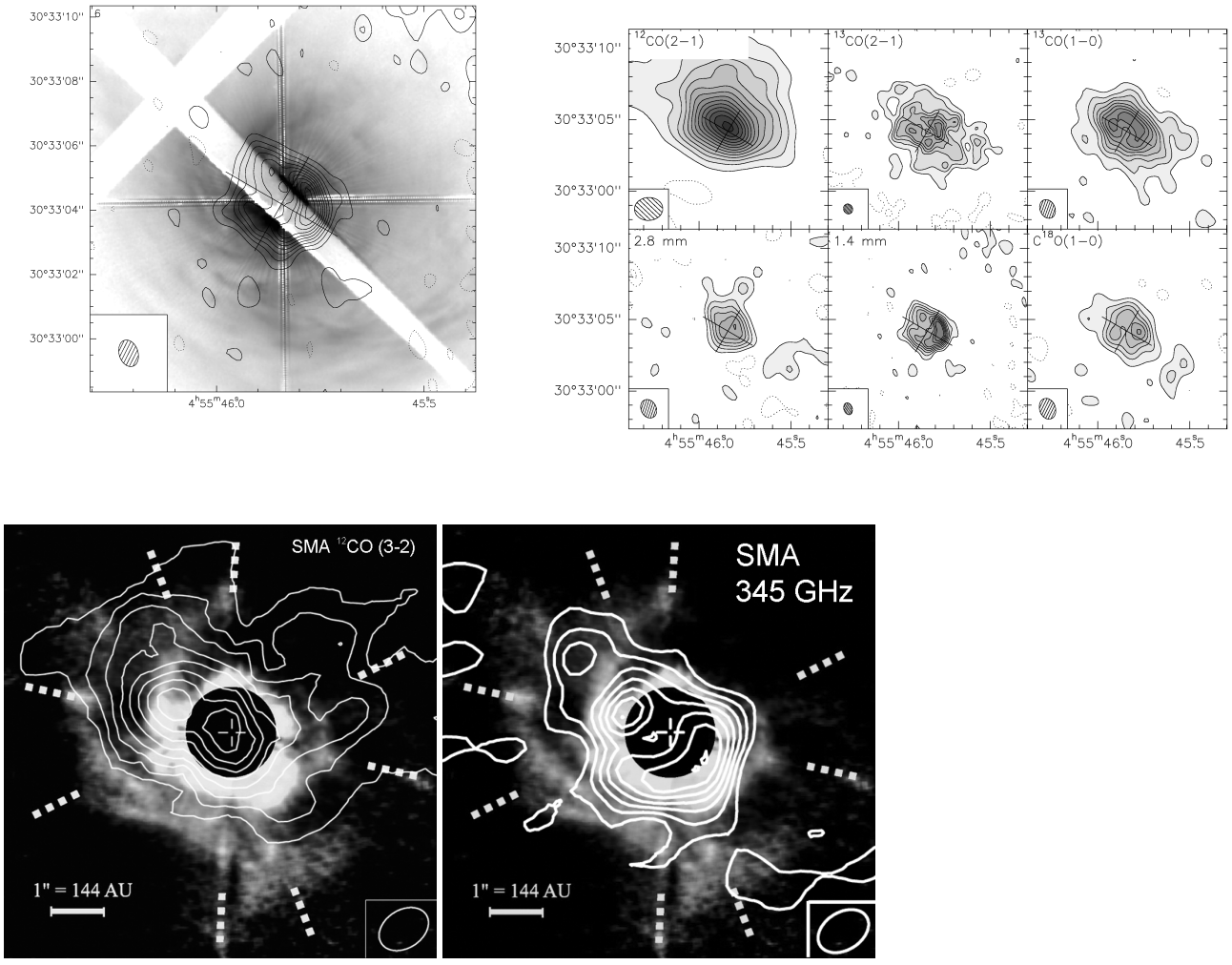

Fig. 7.— Top-Left: 1.4 mm continuum data on AB Aur (in contours) superimposed on the HST image from *Grady et al.* (1999), in false color. The angular resolution is $0.85 \times 0.59''$ at PA 18°. Top-Right: A montage displaying high resolutions image of the continuum emission at 2.8 mm and 1.4 mm, and of the integrated line emission of ^{12}CO J=2→1 ^{13}CO J=2→1 and ^{13}CO J=1→0 transitions. The (lower resolution) emission at 110 GHz is also presented. From *Piétu et al.* (2005). Bottom: Disk of AB Aur observed with the SMA and superimposed to the Subaru Near-Infrared image. Left: CO J=3-2, the angular resolution is $1.04'' \times 0.72''$ (natural weighing). Right: Dust emission, the angular resolution is $0.95'' \times 0.66''$ (obtained by removing the data inside the first 30kλ). The SMA dust images clearly reveal a depression in the center. The sub-mm dust peaks at location of the inner NIR arms. From *Lin et al.* (2006).

formation are required to properly interpret these data.

4.2. TW Hya

Located at a distance of 56 pc, TW Hya is the closest known T Tauri star. With an age of $\sim 5 \cdot 10^6$ years, it is also one of the oldest stars which still exhibits a CO and gas disk *(Kastner et al.*, 1997). Recent observations performed by *Qi et al.* (2004) with the SMA in ^{12}CO J=3-2 confirm that the size of the disk is small with radius ~ 170 AU and show that the disk is not perfectly pole-on but is tilted by $\sim 6^o$ from face-on.

A detailed modelling was performed by *Qi et al.* (2004) on these data. They used 2-D Monte-Carlo codes to constrain the disk properties. Channel maps of the observations and of the best model are shown in Fig. 8. In the modelling, the disk thermal structure was mainly derived from the Spectral Energy Distribution assuming reasonable dust properties, and the gas was assumed to be fully coupled to the dust. While this is a reasonable assumption for the lower CO transitions, the CO J=3-2 line becomes optically thick in a high layer above the disk plane, where the density is not necessarily sufficient to provide full coupling between the gas and dust temperature. The height at which CO J=3-2 becomes optically thick depends significantly on the disk mass and CO abundance, and will vary from one disk to another. Indeed, *Qi et al.* (2004) reported that the

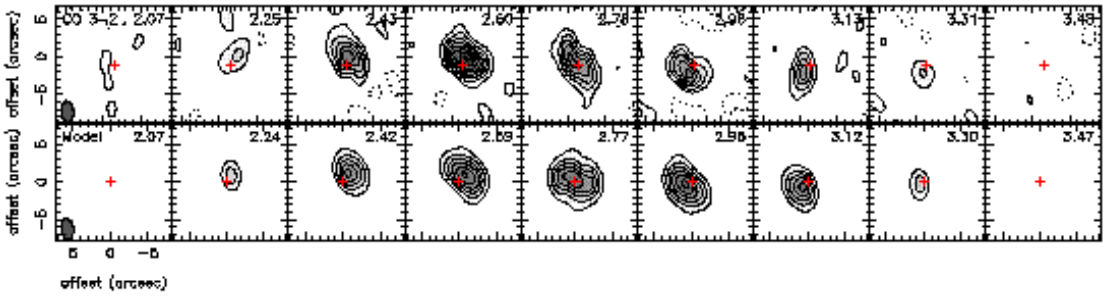

Fig. 8.— Analysis of TW Hya. Channel map for the CO J=3-2 SMA observations (top) and for the best model (bottom). From *Qi et al.* (2004)

predicted CO J=3-2 intensities were always lower than the observed ones, and mentioned that this was most likely due to such an effect.

To check this, *Qi et al.* (2006) used the SMA to map the CO J=6-5 emission in the Tw Hya disk. These new data reveal, like the existing CO J=2-1 and J=3-2 ones, a rotating disk. A detailed simultaneous modelling of the J=3-2 and J=6-5 data show that additional heating is needed to explain the line intensities and that, at least in the outer disk layers, the vertical temperature gradient of the gas is steeper than that of the dust.

A natural heating source is provided by the X-ray emission coming from the star: TW Hya is a strong X-ray emitter with a typical luminosity of $2\,10^{30}$ ergs.s^{-1} *(Kastner et al.*, 1999). Inclusion of an idealized X-ray heating in the disk model provides a better simultaneous fit of the CO J=2-1 and J=3-2 (performed with χ^2 minimization) and also of the J=6-5 data. The agreement with J=6-5 transition is not perfect, but these observations can be considered as the first observed evidence of X-ray heating of molecular gas in T Tauri disks.

4.3. BP Tau

Under many aspects, BP Tau can be considered as the prototype of the CTTS. The object exhibits a high accretion rate of $\sim 3 \cdot 10^{-8}\,\mathrm{M}_\odot$/yr from its circumstellar disk which also produces a strong excess emission in the ultraviolet, visible and NIR *(Gullbring et al.*, 1998). Such a high accretion rate is not surprising since the star is likely very young ($6 \cdot 10^5$yr, *Gullbring et al.*, 1998).

Recent CO J=2-1 and 1.3 mm continuum images obtained with the IRAM array have shown a weak and small CO and dust disk *(Simon et al.*, 2000). The disk is small since its radius is of order $\simeq 120$ AU and in Keplerian rotation around a $(1.3 \pm 0.2)(D/140\mathrm{pc})\,\mathrm{M}_\odot$ mass star. Moreover, contrary to what is observed in other TTauri disks, the detailed analysis of the CO data shows that the J=2-1 transition is marginally optically thin *(Dutrey et al.*, 2003). The disk mass can be estimated from the mm continuum emission by assuming a gas-to-dust ratio of 100, it is very small $\sim 1.2 \cdot 10^{-3}\,\mathrm{M}_\odot$. By reference to this mass, the CO depletion factor is estimated to be ~ 150 with respect to H_2. This CO depletion remains unique compared to other TTauri CO disks, even if one takes into account possible uncertainties such as a lower gas-to-dust ratio or a higher value for the dust absorption coefficient. With a kinetic temperature of about ~ 50 K at 100 AU (derived from the CO data), BP Tau has also the hottest outer disk found so far around a T Tauri star.

One possibility would be that a significant fraction of the disk might be superheated (above the black body temperature) similarly to a disk atmosphere (see model from *Chiang and Goldreich*, 1997). This could explain both the relatively high temperature and the low disk mass. *Dutrey et al.* (2003) have estimated the fraction of small grains ($a \leq 0.1\mu$m) still present in the disk to reach in the visible $\tau_V = 1$ at the disk mid-plane. The mass of small grains is about 10 % of the total mass of dust ($1.2 \cdot 10^{-5}\,\mathrm{M}_\odot$) derived from the mm continuum data.

In view of the TW Hya results, another alternative would be that X-ray (or UV radiation, BP Tau being a very actively accreting object) provides an additional heating of the gas. A more sophisticated modelling, using the appropriate dust and gas densities, would be required to test this idea.

Whatever the cause of the heating, BP Tau remains unique so far for its low CO abundance. It suggests that BP Tau may be a transient object in the phase of clearing its outer disk. This also shows that optical observations alone do not allow comprehensive studies of the disk physics.

5. MOLECULAR CHEMISTRY IN DISKS

Chemistry is an essential agent in the shaping of the gas disks. Molecular (and atomic) abundances play a key role in determining the cooling rate of the gas, and thereby in the thermal balance of the disk. To measure this structure, it is essential to understand where in the disk the molecules are located.

Many examples are given above which illustrate this requirement. Among them, one can cite the process of CO selective photo-dissociation at the disk outer edge in DM Tau *(Dartois et al.*, 2003) or the role of the X-ray heating in the gas disk surface *(Qi et al.*, 2006). Both processes re-

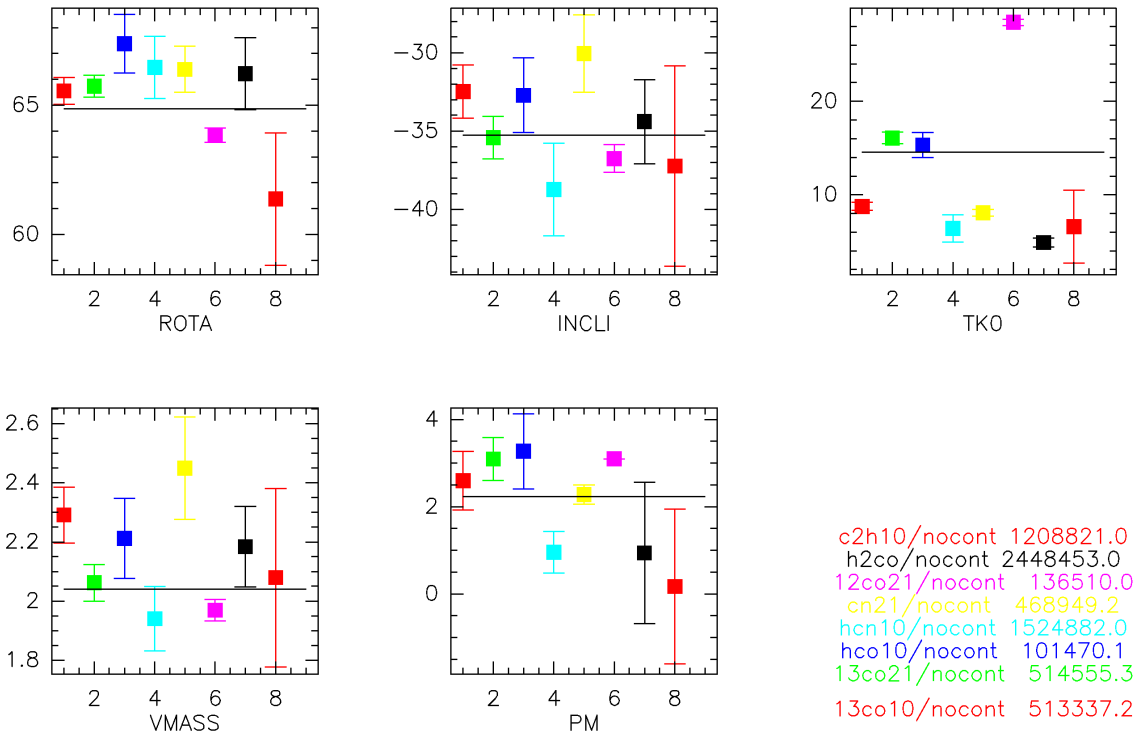

Fig. 9.— Fits of the molecular data obtained with the IRAM PdBI array for DM Tau. From left to right and top to bottom, the parameters are: position angle (ROTA, in ^{o}), inclination (INCLI, in ^{o}), Temperature at 100 AU (TKO, in K), radial velocity at 100 AU, (VMASS, in km/s) and radial index of the surface density law (PM). The good consistency of the error bars on all fits for the geometry and the kinematics clearly demonstrate the robustness of the method and the correct derivation of the error bars. From *Piétu et al.* (2006).

quire a deep understanding of the disk physical structure (at least, the geometry, density and gas and dust temperature) and of the dust properties (e.g. size of dust particles). So far, only the disk geometry can be easily constrained.

Because molecules are in general much less abundant than ^{13}CO, and the line emission much weaker (with the exception of HCO^+ due to its large dipole moment), the sensitivity of the arrays becomes a serious problem for the study of chemistry (see Section 2.3). This explains why so far no comprehensive observational study of the disk chemistry has been published, and that chemical models still refer to the single-dish work of *Dutrey et al.* (1997) or *van Zadelhoff et al.* (2001). Observational studies of the chemistry in disks are currently limited to detections of the more abundant species: HCO^+, CN, C_2H, CS, HCN, H_2CO and DCO^+. The high CN/HCN abundance ratio observed in DM Tau by *Dutrey et al.* (1997), as well as the detection of C_2H, are strongly suggestive of photon-dominated processes.

Another complexity is related to the possible non-LTE effects in the line excitation as discussed in Section 2.6. As a consequence, chemical studies in disks are even more difficult to handle from the point of view of the observations than from the point of view of the theory. A first systematic attempt has been performed by Piétu and collaborators, who recently completed a molecular survey of DM Tau and a few sources including LkCa15 with the IRAM array. Fig. 9 shows the results of the χ^2 minimization, assuming LTE conditions, for the observed molecular transitions in DM Tau. Such an analysis provides a first order indication on the molecular abundance gradients in the disk. Chemical models will have to explain the general trends found e.g. for the HCO^+/CO or CN/HCN ratios, as well as the magnitude of the abundances. However, a detailed comparison with chemical models will require proper incorporation of the disk structure and non-LTE analysis, since some transitions appear sub-thermal.

Note that proper analysis of any line detection in disks require adequate handling of the line formation process, and in particular of the disk kinematics. Failure to do so can result in mis-interpretation of spectral lines, as shown by *Guilloteau et al.* (2006) for HDO in DM Tau. *Guilloteau et al.* (2006) demonstrate that the line-to-continuum ratio of an absorption line from a circumstellar disk is limited to the ratio of intrinsic linewidth (thermal + turbulent) to the projected rotation velocity at the disk edge. Except for edge-on

disks, this ratio is less than about 0.1 – 0.2, showing that the detection of HDO in absorption claimed by *Ceccarelli et al.* (2005) cannot be real.

6. SUMMARY AND PERSPECTIVES

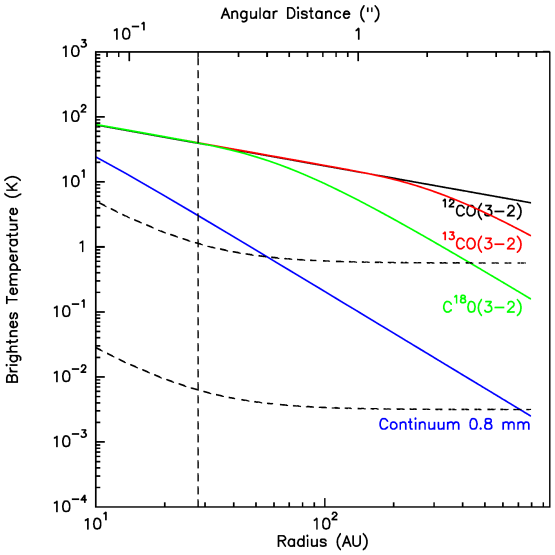

Fig. 10.— Same Figure as Fig. 4 but for ALMA. Brightness temperature for CO (and isotopomers) in J=3-2 transition for a Keplerian disk orbiting a central object of $\sim 1\,M_\odot$ (thick lines) compared to the sensitivity of ALMA with the whole array. Note that the angular resolution is here $0.2''$. This has been done for a T Tauri disk located at the Taurus distance: 140 pc

Mm and sub-mm interferometric studies of spectral lines have revealed a number of essential features of the proto-planetary disks. CO images have shown the existence of large disks, and have been used to constrain stellar masses and disk inclinations, two key parameters for SED modelling. The observations of the CO isotopologues have provided the first direct evidence of the thermal structure of disks, constraining radial and vertical gradients. Although currently biased towards the largest and most isolated disks, observations have also revealed the diversity of the proto-planetary disks. The recent discovery of non-Keplerian rotation around AB Aur may prove important for the understanding of the disk formation process. At the other extreme, objects like BP Tau also indicate that we do not yet understand the causes of the diversity in disk properties.

Because of the intrinsic faintness of the line emission, studies of other molecules than CO isotopologues have not been performed extensively. Large observational projects are now close to completion, and should lead to significant progress in this area in the next years. However, the complexity of the analysis due to the non-LTE line formation process will have to be considered when comparing with chemical models. Significant progress in this area is nevertheless expected, thanks to a combination of several independent improvements:

1. the advent of sub-mm observations with the SMA, which will allow some multi-line studies of molecules, although this will be restricted to very few objects given the sensitivity limitation.

2. the progress in modelling, specially in radiative transfer codes which are now accurate and fast enough to be used systematically

3. the improvement in sensitivity of the mm-arrays which is expected in the next two years, thanks to new dual-polarization receivers of the IRAM PdBI and to the advent of the CARMA array.

4. the improvement in continuum sensitivity, due to increased continuum bandwidth, which will allow better comparisons of dust and gas distributions.

However, sensitivity will remain a concern, and good coordination between the major arrays, as well as use of the best analysis techniques, will be essential to get the best constraints on the chemistry of disks from the available instruments.

Despite these improvements, the studies of molecular disks will largely remain confined to the nearest star formation regions, Taurus-Auriga, TW Hya association and ρ Oph, which are not representative of the bulk of the star formation process. Going beyond this limitation and accessing the nearest star-forming cluster, Orion, will require a further step in sensitivity which can only be provided by ALMA.

ALMA will also allow a major breakthrough in the study of less abundant molecules, such as H_2CO or isotopologues of the other molecules: at the Taurus distance, it will allow meaningful comparison of the distributions of dust and molecules on more than a decade in radius (see Fig. 10.)

Acknowledgments. The SMA is a joint project between the Smithsonian Astrophysical Observatory and the Academia Sinica Institute of Astronomy and Astrophysics, and is funded by the Smithsonian Institution and Academia Sinica. IRAM is supported by INSU/CNRS (France), MPG (Germany) and IGN (Spain). Vincent Piétu and Emmanuel Dartois are acknowledged for many fruitful discussions on proto-planetary disks. Shin-Yi Lin and Chunhua Qi are thanked for providing material for this chapter. Anne Dutrey thanks the CNFA for providing her travel funds to attend PPV. This work was also partially supported by the French "Programme National de Physico-Chimie du Milieu Interstellaire".

References.

D'Alessio P., Canto J., Calvet N., Lizano S. (1998) *Astrophys. J., , 500*, 411-427

D'Alessio P., Calvet N., Hartmann L., Lizano S., and Canto J. (1999) *Astrophys. J., 527*, 893-909

Chiang E. I. and Goldreich P., (1997) *Astrophys. J., 490*, 368-376

Ceccarelli C., Dominik C., Caux E., Lefloch B., and Caselli P. *Astrophys. J., 631*, L81-L84
Dartois E., Dutrey A., and Guilloteau S. (2003) *Astron. Astrophys., 399*, 773-787
Dutrey A., Guilloteau S., and Simon M. (1994) *Astron. Astrophys., 286*, 149-159
Dutrey A., Guilloteau S., and Guélin M. (1997) *Astron. Astrophys., 317*, L55-L58
Dutrey A., Guilloteau S., and Simon M. (2003) *Astron. Astrophys., 402*, 1003-1011
Duvert G., Guilloteau S., Ménard F., Simon M., and Dutrey A. (2000) *Astron. Astrophys., 355*, 165-170
Fukagawa M., Hayashi M., Tamura M., Itoh Y., Hayashi S. S. et al. (2004) *Astrophys. J., 605*, L53-L56
Grady C. A., Woodgate B., Bruhweiler F. C., Boggess A., Plait P. et al. (1999) *Astrophys. J., , 523* L151-L154
Guilloteau S., and Dutrey A. (1994) *Astron. Astrophys., 291*, L23-L26
Guilloteau S., and Dutrey A. (1998) *Astron. Astrophys., 339*, 467-476
Guilloteau S., Pietu V., Dutrey A., and Guélin M. (2006) *Astron. Astrophys., in press*.
Gullbring E., Hartmann L., Briceno C., and Calvet N. (1998) *Astrophys. J., 492*, 323-341
Ho P., Moran J., and Lo K. Y. (2004) *Astrophys. J., 616*, L1-L6
Hogerheijde M. R., and van der Tak F. F. S. (2000) *Astrophys. J., 362*, 697-710
Kastner J. H., Zuckermann B., Weintraub D. A., and Forveille T. (1997) *Science, 277*, 67-71
Kastner J. H., Huenemoerder D. P., Schulz N. S., and Weintraub D. A. (1999) *Astrophys. J., 525*, 837-844
Lin S.Y. et al., (2006) *Astrophys. J., submitted*.
Mannings V., and Sargent A. I. (1997) *Astrophys. J., 490*, 792-802
Mannings V., and Sargent A. I. (2000) *Astrophys. J., 529*, 391-401
Meeus G., Waters L. B. F. M., Bouwman J., van den Ancker M. E., Waelkens C., and Malfait K. (2001) *Astron. Astrophys., 365*, 476-490
Pavlyuchenkov Y. N., and Shustov B. M., 2004, *Astron. Rep. 48*, 315-326
Piétu V., Guilloteau S., Dutrey A., 2005, *Astron. Astrophys., 443*, 945-954
Piétu V. et al. (2006) in preparation
Pringle J. E. (1981), *Ann. Rev. Astron. Astrophys., 19*, 137-162
Semenov D., Pavlyuchenkov Y. N., Schreyer K., Henning T., Dullemond C., and Bacmann A. (2005) *Astrophys. J., 621*, 853-874
Simon M., Dutrey A., and Guilloteau S. (2000) *Astrophys. J., 545*, 1034-1043
Qi C., Ho P. T. P., Wilner D. J., Takakuwa S., Hirano N., et al. (2004) *Astrophys. J., 616* L11-L14
Qi C., Wilner D. J., Calvet N., Bourke T. L., Blake G. A., Hogerheijde M. R., Ho P. T. P., and Bergin E. (2006) *Astrophys. J., 636* L157-L160
van Zadelhoff G.-J., van Dishoeck E. F., Thi W.-F., and Blake G.A. (2001) *Astron. Astrophys., 377*, 566-580